약학석사학위논문

콜라겐 유도 관절염 동물모델과 류마티스 관절염 환자의 조절 T 세포에서 새로운 히스톤 탈아세틸화효소 6 억제제, CKD-L의 치료 효과

Therapeutic effect of a novel histone deacetylase 6 inhibitor, CKD-L, on collagen induced arthritis in vivo and regulatory T cells in rheumatoid arthritis in vitro

2016년 8월

서울대학교 융합과학기술대학원
분자의학 및 바이오제약학과
오보람

Abstract

Therapeutic effect of a novel histone deacetylase 6 inhibitor, CKD-L, on collagen induced arthritis in vivo and regulatory T cells in rheumatoid arthritis in vitro

BO RAM OH
Department of Molecular Medicine and Biopharmaceutical Sciences
The Graduate School
Seoul National University

Background: Epigenetic regulation by histone deacetylase (HDAC) and histone acetyltransferase (HAT) plays an important role in several types of inflammatory arthritis, including rheumatoid arthritis (RA). RA is a chronic autoimmune disease characterized by inflammatory synovitis and progressive destruction of joint cartilage and bone leading to pain, swelling, and loss of function. HDAC inhibitor has recently been reported to have a therapeutic effect as an anti-inflammatory agent in collagen-induced

arthritis (CIA).

Objective: We investigated the therapeutic effect of a new selective HDAC6 inhibitor, CKD-L, compared to ITF 2357 or Tubastatin A on CIA and regulatory T (Treg) cells in patients with RA.

Methods: CIA was induced by bovine type II collagen (CII) in DBA/1J mice. Mice were treated with vehicle (n=10), CKD-L (15 or 30 mg/kg, n=10, respectively), or Tubastatin A (30 mg/kg, n=9) by subcutaneous injection every day for 18 days. Arthritis score was assessed twice weekly after the onset of arthritis. Histological analysis was performed by H&E stain.
$CD4^+CD25^-$ T cells were isolated from splenocytes of naive C57BL/6 mice and incubated with anti-CD3/CD28 beads, TGF-β and HDAC6 inhibitor (1 to 10 μM) for 6 days. Cytotoxic T lymphocyte associated protein 4 (CTLA-4) expression in induced Treg cells was analyzed by flow cytometry.

RA PBMCs were cultured in the presence of 100 ng/ml lipopolysaccharide with or without HDAC inhibitor (CKD-L and Tubastatin A, 0.01 to 5 μM, ITF 2357, 0.01 to 0.1 μM) for 24 hours. The secretions of TNF-α, IL-10, IL-1β and IL-6 in the culture

supernatant were measured by ELISA. TNF-α and IL-10 mRNA expression levels were analyzed by real-time PCR.

THP-1 cells were activated with PMA for 24 hours to induce macrophage differentiation. PMA-activated THP-1 was treated with vehicle or HDAC inhibitor (0.1 to 10 μM) for 24 hours and then with 100 ng/ml of LPS for 4 hours. The secretion of TNF-α was measured by ELISA.

$CD4^+CD25^-$ T cells from RA patients were cultured with anti-CD3 antibody, anti-CD28 antibody, IL-2, TGF-β, and 1,25-dihydroxyvitamin D_3 for 5 days. Induced Treg cells were incubated for 3 days with 5 μM carboxyfluorescein succinmidyl ester (CFSE)-Teff cells in the presence of anti-CD3/CD28 beads and HDAC inhibitor (ITF 2357, 0.01 to 0.1 μM, CKD-L and Tubastatin A, 0.01 to 5 μM). The proliferation of Teff cells was analyzed by flow cytometry.

Result: In the CIA model, CKD-L and Tubastatin A significantly decreased arthritis score (CKD-L, $p < 0.05$; Tubastatin A, $p < 0.01$) and histological score (CKD-L and Tubastatin A, both $p < 0.001$). CTLA-4 expression in $Foxp3^+$ T cells was significantly increased after treatment with CKD-L ($p < 0.001$) and

Tubastatin A ($p < 0.05$).

In RA PBMC, CKD-L significantly inhibited TNF-α and IL-1β, and increased IL-10. ITF 2357 and Tubastatin A inhibited TNF-α, but had no effect on IL-1β or IL-10. IL-6 was not altered by treatment with any HDAC inhibitor. CKD-L ($p < 0.01$), ITF 2357 ($p < 0.001$), and Tubastatin A ($p < 0.001$) significantly inhibited TNF-α mRNA expression.

TNF-α secretion from PMA-activated THP-1 cells was reduced after treatment with CKD-L ($p < 0.001$) and Tubastatin A ($p < 0.001$).

When induced Treg cells and Teff cells, the proliferation of Teff cells was significantly inhibited after treatment with CKD-L 5 μM ($p < 0.05$) and ITF 2357 0.1 μM ($p < 0.001$) compared to vehicle. As the proportion of induced Treg cells increased, Teff cell proliferation was inhibited to a greater degree. Tubastatin A had no effect on inhibition of proliferation.

Conclusion: CKD-L, a selective HDAC6 inhibitor, decreased arthritis score in CIA, reduced the expression of TNF-α and IL-1β, and increased the expression of IL-10 in PBMC from RA patients. CKD-L increased CTLA-4 expression and the

suppressive function of Treg cells. These results suggest that CKD-L may have a beneficial effect in the treatment of rheumatoid arthritis.

Key words: histone deacetylase 6, histone deacetylase inhibitor, rheumatoid arthritis, collagen induced arthritis, regulatory T cell

Student number: 2011-24246

Contents

List of figures

List of abbreviations

ACR: American College of Rheumatology

BSA: bovine serum albumin

CD4: cluster of differentiation 4

CD25: cluster of differentiation 25

cDNA: complementary DNA

CFA: complete Freund’ s adjuvant

CFSE: carboxyfluorescein succinimidyl ester

CIA: collagen induced arthritis

CTLA-4: cytotoxic T lymphocyte antigen-4

dNTP: deoxynucleotide triphosphate

DMARDs: disease-modifying antirheumatic drugs

DMSO: dimethyl sulfoxide

EDTA: ethylenediaminetetraacetic acid

ELISA: enzyme-linked immunosorbent assay

FBS: fetal bovine serum

FLS: fibroblast-like synoviocyte

Foxp3: forkhead box P3

HAT: histone acetyltransferase

HDAC: histone deacetylase

H&E: hematoxylin and eosin

HSP 90: heat shock protein 90

IFA: incomplete Freund’ s adjuvant

IFN-γ: interferon-gamma

IL-1β: interleukin-1 beta

IL-2: interleukin-2

IL-6: interleukin-6

IL-10: interleukin-10

LPS: lipopolysaccharide

MACS: magnetic cell sorting

MTT: methylthiazol tetrazolium

MTX: methotrexate

NAD: nicotinamide adenine dinucleotide

NSAIDs: nonsteroidal anti-inflammatory drugs

PBMCs: peripheral blood mononuclear cells

PBS: phosphate-buffered saline

PMA: phorbol 12-myristate 13-acetate

PRX: peroxiredoxin

P/S: penicillin streptomycin

RA: rheumatoid arthritis

RT: room temperature

RT-PCR: reverse transcription-polymerase chain reaction

Teff cells: effector T cells

TGF-β: transforming growth factor beta

TNF-α: tumor necrosis factor alpha

Treg cells: regulatory T cell

Introduction

Histone deacetylase (HDAC) and histone acetyltransferase (HAT) play important roles in the regulation of gene transcription [1]. The positively charged lysine in the N-terminal tail of histones is neutralized by acetylation of histone by HAT, and the binding affinity between the DNA backbone and histones is decreased because histones do not bind to the negatively charged phosphate groups in DNA. The decreased level of interaction between DNA and histones increases gene transcription by promoting the binding of transcription factors to DNA [2-4].

In opposition to HAT, deacetylation of histone by HDAC represses gene transcription through chromatin condensation [5]. HDAC is classified into 4 classes based on DNA sequence similarity and function. Class I, II, and IV HDACs are classical HDACs that have a zinc-dependent active site, whereas class III HDACs are a family of nicotinamide adenine dinucleotide (NAD^+)-dependent proteins. Class I HDACs (HDACs 1-3 and 8) are primarily found in the nucleus and class II HDACs (HDAC4-7, 9 and 10) are found in both the nucleus and the cytoplasm and can shuttle between the

two. The class IV HDAC (HDAC11) shares structural similarities with both class I and class II HDACs. Class III HDACs (SirT1-7) have distinct structures and different mechanisms of action. Their enzymatic activity depends on the cofactor NAD^+ [1, 6, 7].

HDAC6 is primarily located in the cytoplasm and has a unique structure that contains two homologous catalytic domains and an ubiquitin binding domain at the C-terminal end [8, 9]. HDAC6 has been reported to involve many important biological processes, including cell migration, immune response, viral infection and the degradation of misfolded proteins. The substrates of HDAC6 are α-tubulin, heat shock protein 90 (HSP 90), peroxiredoxin (PRX), and cortactin, and HDAC6 regulates acetylation of multiple proteins by forming various complexes with other partner proteins. These diverse functions of HDAC6 offer potential therapeutic targets in various diseases such as systemic lupus erythematosus, cancer and diabetes [10, 11]. The inhibition of HDAC6 was reported to enhance the suppressive activity of regulatory T (Treg) cells in inflammation and autoimmunity [12].

Histone deacetylase inhibitors modulate the function of HDACs and activate and/or repress gene expression. HDAC inhibition leads to cell cycle arrest, cell growth,

cell differentiation, and apoptotic death of transformed cells [13, 14]. HDAC inhibitors have been developed. The pan HDAC inhibitors such as ITF 2357 and SAHA, inhibit all HDACs and the selective HDAC inhibitors such as Tubastatin A and Tubacin, inhibit HDAC6 specifically [15].

Epigenetic regulation plays an important role in inflammatory autoimmune diseases including rheumatoid arthritis (RA) through changes in histone modification [16]. RA is a chronic autoimmune disease characterized by inflammatory synovitis and progressive destruction of joint cartilage and bone leading to swelling, pain, stiffness, and loss of function [17, 18]. The etiology of RA remains unclear, but genetic background and environmental factors play important roles in the disease [19].

Current medical treatments for RA include nonsteroidal anti-inflammatory drugs (NSAIDs) and disease-modifying antirheumatic drugs (DMARDs), including methotrexate (MTX), sulfasalazine, and tumor necrosis factor-α (TNF-α) inhibitors (infliximab, etanercept, and adalimumab) [20]. TNF-α is a pro-inflammatory cytokine that is associated with the development of RA. TNF-α blockade can be an effective treatment for RA [21]. However, about 40%

of RA patients do not respond to anti-TNF-α therapy, so novel therapies are required for patients who show no response [1, 5].

HDAC inhibitors have been reported to have potential therapeutic effects as anti-inflammatory agents in many studies including those on collagen-induced arthritis (CIA) [5, 22-25]. HDAC inhibitors suppressed the production of IL-6 in RA fibroblast-like synoviocytes (FLS) and macrophages by promoting mRNA decay [26]. In RA, macrophages and T cells are major sources of pro-inflammatory cytokines [27]. The activation, survival, and apoptosis of macrophages are regulated by acetylation and deacetylation of histones. HDAC inhibitors suppress TNF-α and IL-6 production and cytokine gene transcription and induce apoptosis in macrophages [28].

HDAC inhibitors reduce the secretion of pro-inflammatory cytokines, such as TNF-α and IL-6, in peripheral blood mononuclear cells (PBMCs) of RA patients and reduce the secretion of TNF-α, IL-1α, IL-1β, and interferon-gamma (IFN-γ) in lipopolysaccharide (LPS)-stimulated normal PBMCs [1, 24]. Treg cells are a subset of $CD4^+$ T cells that have an immunosuppressive role in immune tolerance [29]. Treg cells from RA patients are defective in

suppressing pro-inflammatory cytokine production [30].

CKD-L is a new HDAC6 inhibitor developed by the Chong Kun Dang Pharmaceutical Corporation. We investigated the therapeutic effect of the novel selective HDAC6 inhibitor, CKD-L, and compared its effect to those of the pan HDAC inhibitor, ITF 2357 and the selective HDAC6 inhibitor, Tubastatin A in CIA, PBMCs, and Treg cells from patients with RA.

Material and method

1. Chemicals

CKD-L is a new histone deacetylase 6 inhibitor developed by the Chong Kun Dang Pharmaceutical Corporation (CKD Pharm). ITF 2357 and Tubastatin A were also provided by CKD Pharm and were used as positive controls (pan HDAC inhibitor and selective HDAC6 inhibitor, respectively). These chemicals were dissolved in dimethyl sulfoxide (DMSO; Sigma-Aldrich, St. Louis, MO, USA). The stock solutions were stored at -20℃ and were diluted to the required concentrations in growth media as necessary. Vehicle (DMSO) was used in the negative control groups.

2. Animals

DBA/1J mice (male, 6 weeks old) and C57BL/6 mice (male, 6 weeks old) were purchased from Central Lab Animal, Inc. (SLP, Hamamatsu, Japan). The animals were kept in a specific pathogen-free facility. The animals were provided with standard diet and water ad libitum.

3. CIA experiments

Before the first immunization, bovine type II collagen (CII) (Chondrex, Redmond, WA) 2 mg/ml in 0.05 M acetic acid and an equal volume of complete Freund's adjuvant (CFA) (Chondrex) were mixed by using a pre-cooled homogenizer in an ice bath. 100 μl of the emulsion was injected intradermally at the base of the tail of each DBA1/J mouse on day 1.

On day 21 after the first immunization, the mice were boosted with the second immunization. Bovine type II collagen (2 mg/ml in 0.05 M acetic acid) and an equal volume of incomplete Freund's adjuvant (IFA) (Condrex) were mixed by using a pre-cooled homogenizer in an ice bath. 100 μl of the emulsion was injected intradermally at the base of the tail of each mouse.

3.1. Drug administration and evaluation of arthritis

After the second immunization, the mice were divided into 4 equal groups on the basis of their body weight and given either vehicle or HDAC6 inhibitors. CKD-L and Tubastatin A were dissolved in cremophor EL:ethanol:saline=1.5:1.5:7. Mice were treated with vehicle (n=10), CKD-L (15 or 30 mg/kg, n=10 for both) or Tubastatin A (30 mg/kg, n=9) by subcutaneous injection every day for 18 days. Arthritis score and

body weight were assessed every two days after the first drug administration. On day 38, all mice were sacrificed after anaesthetization for pathological analysis.

3.2. Arthritis score assessment

Arthritis score was evaluated as 5 scales as previously reported [31].

0: No evidence of erythema and swelling

1: Erythema and mild swelling confined to the tarsals or ankle joint

2: Erythema and mild swelling extending from the ankle to the tarsals

3: Erythema and moderate swelling extending from the ankle to metatarsal joints

4: Erythema and severe swelling encompass the ankle, foot and digits, or ankylosis of the limb

Arthritis was scored using a scale of 0-4 for each paw. The total score per mouse was summed from 0 to 16 (normal: 0, maximum severe score: 16).

3.3. Body weight change (%) after onset of arthritis

Change in body weight is a general marker of various diseases including RA. Thus, body weight change after onset of arthritis can reflect disease

progression.

3.4. Histological score

The knee joints and hind paws of mice in each group were dissected for histopathological analysis. Dissected knee joints and hind paws were fixed in 10% phosphate-buffered formalin (pH 7.4), decalcified in 10% ethylenediamine tetraacetic acid (EDTA) for ~2 weeks, embedded in paraffin, and then as per standard methods. The sections were stained with hematoxylin and eosin (H&E) and scored by seven independent, blinded observers. Synovial inflammation, bone erosion, cartilage damage, and leukocyte infiltration were assessed using a scale of 0-4 (normal: 0, mild: 1, moderate: 2, marked: 3, severe: 4). Histological score was calculated by summation of these scales (normal: 0, maximum score: 16).

4. Cytotoxic T lymphocyte antigen-4 (CTLA-4) expression using induced murine Treg cells

4.1. Cell preparation and enzymatic digestion

Spleens from naive C57BL/6 mice were harvested and then incubated with 2 mg/ml collagenase D (Roche, Mannheim, Germany) for 30 minutes at 37℃. Spleens were meshed through a 70 μm cell strainer (Becton

Dickinson, Franklin Lakes, NJ) to obtain single cell suspensions.

Treg cells ($CD4^+CD25^+$ T cells) and effector T (Teff) cells ($CD4^+CD25^-$ T cells) were isolated from splenocytes using a $CD4^+CD25^+$ regulatory T Cell Isolation Kit (Miltenyi Biotec) by magnetic cell sorting (MACS) separator according to the manufacturer's instructions. The purity of each cell population (> 95%) was confirmed by flow cytometry.

4.2. Treg cell induction and drug treatment

$CD4^+CD25^-$ T cells were isolated from splenocytes using the $CD4^+CD25^+$ regulatory T Cell Isolation Kit (Miltenyi Biotec) as a negative fraction by MACS separator. The purity of the isolated cell population (> 95%) was confirmed by flow cytometry.

$CD4^+CD25^-$ T cells ($5X10^5$ cells/ml/well) were incubated with vehicle or HDAC6 inhibitor (1 to 10 μM) in the presence of anti-CD3/CD28 beads (T cell Activation/Expansion kit, Miltenyi Biotec), and recombinant mouse transforming growth factor beta (TGF)-β2 (R&D systems Inc., Minneapolis, MN, 40 pg/ml) in a 48 well plate (Becton Dickinson) for 6 days at 37℃ in a humidified 5% CO_2 incubator.

For surface staining, cells were incubated with

PE-Cy7-labeled anti-mouse CD4 (eBioscience), and APC-labeled anti-mouse CD25 (eBioscience) for 20 min at room temperature (RT). For intracellular staining, the cells were fixed and permeabilized with fix/permeabilization buffer (eBioscience) for 20 min at 4℃, washed twice with wash buffer and then incubated with AlexaFluor488-labeled anti-mouse forkhead box P3 (Foxp3) and PE-labeled anti-mouse CTLA-4 (eBioscience) for 20 min at 4℃ in the dark. CTLA-4 expression of induced $Foxp3^+$ Treg cells was analyzed by FACSCantoII flow cytometry (BD bioscience) and the results were analyzed with FlowJo software (TreeStar Inc. Ashland, OR, USA).

5. RA patients

5.1. RA patients and healthy controls

Patients with RA were enrolled at the Rheumatology Clinic, Seoul National University Hospital. All RA patients fulfilled the 1987 American College of Rheumatology (ACR) classification criteria of RA [32]. Healthy controls were volunteers that did not have rheumatoid arthritis. This study was approved by the Institutional Review Board and informed consent was obtained from each patient.

5.2. Methylthiazol tetrazolium (MTT) assay and cell viability

Heparinized blood of RA patients was diluted with an equal volume of phosphate-buffered saline (PBS), and diluted whole blood was carefully layered over Ficoll-Paque™ PLUS (specific gravity 1.007 g/ml, GE Healthcare Life Science, Uppsala, Sweden) (blood:PBS:Ficoll:=1:1:1). After centrifugation at 1700 rpm for 30 minutes at RT, PBMCs were isolated from the plasma and Ficoll interface and washed twice with PBS.

Isolated PBMCs were cultured in a 96 well plate and treated with LPS (100 ng/ml) (Sigma-Aldrich) and vehicle or HDAC inhibitor (0.01 to 5 μM) in RPMI 1640 media containing 10% (v/v) FBS and 1% penicillin/streptomycin (P/S; 10,000 units/ml, Gibco/BRL, Grand Island, NY, USA) for 24 hours at 37℃ in a humidified 5% CO_2 incubator. For the MTT assay, 10 μl of CCK-8 solution (CCK-8; Dojindo Laboratory, Kumamoto, Japan) was added to each well and incubated for 2 hours at 37℃ in the dark. The absorbance in solution was measured by a Luminex 200 (Luminex Corporation, Austin, TX, USA) at 450 nm.

5.3. Cytokine assay

Isolated PBMCs were cultured in a 48 well plate (Becton Dickinson) and treated with LPS (100 ng/ml) and vehicle or HDAC inhibitor (0.01 to 5 μM) in RPMI 1640 media containing 10% FBS and 1% P/S for 24 hours at 37℃ in a humidified 5% CO_2 incubator. Cell culture supernatant was harvested for multiplex immunoassay of TNF-α, IL-1β, and IL-10 using Bio-Plex Pro™ Assay (Bio-Rad Laboratories, Hercules, CA, USA), according to the manufacturer's instructions. The secretion of IL-6 in the cell culture supernatant was measured by using the Human IL-6 DuoSet enzyme-linked immunosorbent assay (ELISA) kit (R&D) according to the manufacturer's instructions.

5.4. RNA preparation

Cells were harvested and washed with PBS for RNA preparation. Total RNA was extracted by using an RNeasy micro kit (Qiagen, Valencia, CA, USA) according to the manufacturer's instructions. In brief, 350 μl of RLT buffer was added to the pelleted cells ($5X10^5$ cells) to lyse them. An equal volume of 70% ethanol was added to the lysate and gently mixed by pipetting. The mixed lysate was transferred into an RNeasy MinElute spin column placed in a 2 ml

collection tube and centrifuged at 8000 g for 15 seconds at RT. After washing with 350 μl of RW1 buffer, 80 μl of DNase I working solution was added directly to the column membrane and incubated for 15 minutes at RT. After washing with 350 μl of RW1 buffer, 500 μl of RPE buffer was added to the column, which was centrifuged at 8000 g for 15 seconds at RT. 500 μl of 80% ethanol was added to the column and centrifuged at 8000 g for 2 minutes at RT. The column was transferred in a new 1.5 ml collection tube and 14 μl of RNase-free water was directly added to the center of the column membrane. The column was centrifuged at full speed for 1 minute at RT to elute the RNA. The concentration of RNA was determined by measuring absorbance at 260 nm with a Nanodrop ND-100 spectrometer (Nanodrop Technologies, Wilmington, DE, USA).

5.5. Reverse transcription-polymerase chain reaction (RT-PCR) and complementary DNA (cDNA) synthesis

First-strand cDNA was synthesized from an equal concentration of total RNA by using the SuperScript® Ⅲ First-Strand Synthesis System (Invitrogen, Carlsbad, CA, USA). The reaction was conducted in a final volume of 10 μl containing 20 ng of total RNA, 5 μM

oligo (dT)20 primer and 1 mM deoxynucleotide triphosphate (dNTP) mixture in a 200 ㎕ tube. The tube was incubated for 5 minutes at 65℃ and placed on ice for at least 1 minute. A cDNA synthesis mix solution was prepared with 10X RT buffer, 10 mM DTT, 50 mM $MgCl_2$, 2 units of RNaseOUT and 10 units of SuperScript® Ⅲ RT. 10 ㎕ of that mix solution was added to each reaction mixture, mixed gently, and incubated for 50 minutes at 50℃ and for 5 minutes at 85℃, then placed on ice. To remove the remaining RNA, 1 ㎕ of RNase H was added to each reaction mixture for 20 minutes at 37℃ before. RT-PCR was performed with a PTC 200 thermal cycler (MJ research Inc., Waltham, Ma, USA).

5.6. cDNA pre-amplification

cDNA was amplified using a Taqman PreAmp Master Mix (Applied Biosystems, Foster City, CA, USA) according to the manufacturer's instructions. In brief, 10 ㎕ of 20X Taqman gene expression assay was added to a tube and Tris-EDTA buffer was added to be 1 ml of total volume. The reaction was performed in a final volume of 50 ㎕ containing 12.5 ㎕ of synthesized cDNA, 5 ㎕ of 2X Taqman preamp master mix, 12.5 ㎕ of 0.2X pooled assay mix and 20 ㎕ of nuclease-free

water. The reactions were incubated for 10 minutes at 95℃ for one cycle, and then for 15 seconds at 95℃ and 4 minutes at 65℃ for 10 cycles. The amplified products were used after being diluted with Tris-EDTA buffer at a ratio of 1:5 before real-time PCR.

5.7. Quantitative real-time PCR

Quantitative real-time PCR was performed by running a Taqman probe in an ABI 7500 real-time PCR system (Applied Biosystems, Foster Ctiy, CA, USA) according to the manufacturer's instructions. Human IL-10 (Hs00961622, Applied Biosystems), TNF-α (Hs01113624), and 18S (Hs99999901)-specific probes were purchased from Applied Biosystems.

The reaction was performed in a final volume of 20 μl containing 5 μl of diluted amplified cDNA, 1 μl of 20X Taqman gene expression assay buffer, 10 μl of 2X Taqman gene expression master mix, and 4 μl of nuclease-free water. The reactions were incubated for 15 minutes at 94℃ for one cycle and then at 94℃ (15 seconds), 59℃ (30 seconds) and 72℃ (30 seconds) for 40 cycles. The quantity of target gene was calculated by the difference between the target gene and reference gene in the threshold cycle (Ct). Relative gene expression was determined using the $2^{-\Delta\Delta Ct}$

method by normalizing with 18S as a reference gene.

6. TNF-α secretion in phorbol 12-myristate 13-acetate (PMA)-activated THP-1 cells

THP-1 cell is a human monocytic cell line, and PMA-activated THP-1 releases the inflammatory cytokine TNF-α. THP-1 cells were cultured in a 24 well plate ($1X10^5$ cells/well) and activated with PMA (10 ng/ml) (Sigma-Aldrich) in RPMI 1640 media containing 10% FBS and 1% P/S for 24 hours to induce macrophage differentiation. Cells were washed with PBS, treated with vehicle or HDAC inhibitor (0.1 to 10 μM) for 24 hours, and then treated with 100 ng/ml LPS for 4 hours in a humidified 5% CO_2 incubator. The cell culture supernatant was harvested and TNF-α secretion was measured using a TNF-α ELISA kit (eBioscience) according to the manufacturer's instructions.

7. Induction of Treg cells from PBMCs of RA patients

7.1. Isolation of $CD4^+CD25^-$ T cells

$CD4^+CD25^-$ T cells were isolated from PBMCs of RA patients by MACS separator according to the manufacturer's instructions. In brief, PBMCs were incubated with a cocktail of biotin-conjugated

monoclonal anti-human antibodies; CD8, CD14, CD15, CD16, CD19, CD36, CD56, CD123, TCRγ/δ, and CD235a (Glycophorin A) in MACS buffer (PBS, 0.5% bovine serum albumin and 2 mM EDTA, pH 7.2) for 10 minutes at 4℃ in the dark. Then, cells were incubated with anti-biotin microbead for 15 minutes at 4℃. Non-$CD4^+$ cells were indirectly magnetically labeled using a cocktail of biotin-conjugated antibodies as primary reagent and anti-biotin monoclonal antibodies conjugated to microbead as secondary reagent. The labeled cells were removed as a negative fraction using an LD column. Isolated $CD4^+$ cells were incubated with microbead conjugated to a monoclonal anti-human CD25 antibody (MACS®; Miltenyi Biotec) for 15 minutes at 4℃. The labeled cells were removed as a negative fraction using an LD column. The purity of isolated $CD4^+CD25^-$ T cells was > 95% as confirmed by flow cytometry.

7.2. Induction of Treg cells

Anti-human CD3 antibody (eBioscience) 200 μl (2 μg/ml PBS) was added to each well of a 48 well plate. After being sealed, the plate was incubated overnight at 4℃. The coated plate was washed twice with PBS before seeding. $CD4^+CD25^-$ T cells were cultured with

2 μg/ml of anti-human CD28 antibody (BD Pharmingen, San Diego, CA, USA), 2 ng/ml of IL-2 (Peprotech, London, UK), 5 ng/ml of TGF-β (Peprotech, London, UK), and 20 nM of 1,25-dihydroxyvitamin D_3 (Sigma-Aldrich) in X-VIVO™ 15 media (Lonza, Walkersville, MD, USA) containing 1% P/S and 10% heat-inactivated human serum AB (Lonza) for 5 days at 37℃ in a 5% CO_2 incubator. Induced Treg cells were harvested and washed with PBS. Cells were cultured in X-VIVO™ 15 media containing 20 ng/ml of IL-2 in a new 48 well plate for 2 days. The phenotype of induced Treg cells was confirmed by flow cytometry using PerCP-labeled anti-human CD4 antibody, PE labeled anti-human CD25 antibody, APC-labeled anti-human Foxp3 antibody and PE-Cy5-labeled anti-human CTLA-4 antibody.

7.3. Suppression assay

Teff cells ($CD4^+CD25^-$ T cells) were isolated from PBMCs of heathy volunteers by MACS separator and labeled with a CellTrace™ Carboxyfluorescein succinimidyl ester (CFSE) cell proliferation kit (Celltrace, Molecular Probes, Invitrogen) according to the manufacturer's instructions. In brief, isolated Teff cells were resuspended in pre-warmed PBS containing

0.1% bovine serum albumin (BSA; Sigma-Aldrich) at a final concentration of $1X10^6$ cells/ml. Teff cells were labeled by CFSE solution at 5 mM of the final working concentration for 10 minutes at 37℃ in the dark. CFSE-labeled Teff cells were added to 5X volume of cold culture media and placed on ice for 5 minutes to stop the labeling process. Induced Treg cells were mixed with CFSE-labeled Teff cells at ratios of 1:1, 0.3:1 and 0:1 to produce a total cell count per well of $5X10^4$/200 ㎕ RPMI 1640 media containing 1% P/S and 10% FBS in a 96 well plate. The mixed cells were incubated with vehicle or HDAC inhibitor (0.01 to 5 ㎛ M) in the presence of Dynabeads® human T-activator CD3/C28 (one bead to 4 cells) for 3 days in the dark in a humidified 5% CO_2 incubator. Proliferation of Teff cells was analyzed by CFSE dilution using LSR II flow cytometry (BD Bioscience). The results were analyzed with FlowJo software. The suppression ratio was calculated using the fold inhibition of cell proliferation by HDACi vs. vehicle when the ratio of Treg:Teff=1:1.

8. Statistical analysis

Statistical analysis was carried out with GraphPad Prism 5 (GraphPad Software Inc., San Diego, CA, USA). All data were expressed as mean ± SEM. One

way ANOVA followed by Dunnett's multiple comparison tests and Mann-Whitney U tests were used to compare differences between groups. A p value < 0.05 was considered statistically significant.

Result

We assessed the therapeutic effects of CKD-L on the severity of CIA in DBA1/J mice. After the onset of CIA, HDAC inhibitors were administrated by subcutaneous injection. Arthritis progressed rapidly in group treated with vehicle. CKD-L (30 mg/kg) significantly decreased the severity of arthritis compared with vehicle (p <0.05), and Tubastatin A had a similar effect (Fig 1a). The arthritis scores of the mice treated with 30 mg/kg of CKD-L tended to be lower than those of the mice treated with 15 mg/kg of CKD-L. Body weight was assessed every two days after the first drug administration. The body weights of the animals did not change significantly after administration of HDAC inhibitor (Fig 1b). The changes in body weight between the first (day 21) and the last (day 38) assessment were not significantly different among the groups (Fig 1c).

RA is characterized by synovial inflammation, bone erosion, cartilage damage and leukocyte infiltration in the joints. To investigate the protective effects of CKD-L in the joints, histological score was assessed in the knees and hind paws of mice by H&E staining.

Significantly more synovial inflammation, bone erosion, cartilage damage, and leukocyte infiltration were observed in the knee joints and hind paws of the mice treated with vehicle (arrow) compared to Tubastatin A or CKD-L (Fig 2a). CKD-L effectively inhibited arthritis. Synovial inflammation (Fig 2b), bone erosion (Fig 2c), cartilage damage (Fig 2d), and leukocyte infiltration (Fig 2e) were significantly decreased in the groups treated with CKD-L or Tubastatin A compared to the vehicle-treated group. The histological score was calculated by summation of four parameters, synovial inflammation, bone erosion, cartilage damage, and leukocyte infiltration (Fig 2f). Histological score was significantly less in mice treated with CKD-L ($p < 0.001$) or Tubastatin A ($p < 0.001$). These findings suggest that CKD-L may be significantly effective for the treatment of CIA. There was no significant difference of histological score between Tubastatin A and CKD-L.

Treg cells have an immunosuppressive role [29]. It was reported that the suppressive function of Treg cells in RA patients is defective [30, 33]. We assessed the effect of CKD-L on Treg cells during their induction. $CD4^+CD25^-$ T cells were isolated from splenocytes of C57BL/6 mice. $CD4^+CD25^-$ T cells were

incubated with vehicle or HDAC6 inhibitor (1 to 10 μM) in the presence of anti-CD3/CD28 beads and recombinant TGF-β2 in a 48 well plate for 6 days. CTLA-4 expression in $CD4^+CD25^+Foxp3^+$ T cells was significantly increased after treatment with CKD-L ($p < 0.001$) or Tubastatin A ($p < 0.05$) compared to vehicle (Fig 3).

To investigate the effect of CKD-L on PBMCs of RA patients, cell viability was determined using the MTT assay. Cell viability was not affected by high concentrations of CKD-L or Tubastatin A (Fig 4). However, ITF 2357 decreased cell viability at concentrations above 1 μM. The HDAC inhibitors were used in the experiments at concentrations that would not affect cell viability.

Isolated PBMCs from RA patients were cultured with LPS (100 ng/ml) and HDAC inhibitors at different concentrations (0.01 to 5 μM) for 24 hours. The secretions of TNF-α, IL-10, and IL-1β in the cell culture supernatant were measured by multiplex immunoassay and IL-6 secretion in the cell culture supernatant was measured by ELISA. CKD-L significantly inhibited TNF-α at concentrations of 0.01 μM and 5 μM (Fig 5a). Also, CKD-L inhibited IL-1β at a concentration of 1 μM (Fig 5b) and

increased IL-10 at a concentration of 5 μM (Fig 5d). ITF 2357 inhibited TNF-α at a concentration of 0.1 μM and Tubastatin A inhibited TNF-α at concentrations of 1 μM and 5 μM. ITF 2357 and Tubastatin A had no effect on IL-1β and IL-10. IL-6 production did not change following treatment with any HDAC inhibitor (Fig 5c).

Real-time PCR was conducted to measure the mRNA levels of TNF-α and IL-10. Total RNA was extracted from harvested cells and cDNA was synthesized by RT-PCR and then amplified. TNF-α mRNA expression was significantly decreased after treatment with a high concentration (5 μM) of CKD-L ($p < 0.001$) (Fig 6). ITF 2357 and Tubastatin A also decreased TNF-α mRNA expression ($p < 0.001$). However, IL-10 mRNA levels did not change after treatment with CKD-L.

THP-1 cells were activated with PMA for 24 hours to induce macrophage differentiation. After differentiation, they were treated with vehicle or HDAC inhibitor (0.1 to 10 μM) for 24 hours and then treated with 100 ng/ml LPS for 4 hours. TNF-α was significantly decreased after treatment with CKD-L in a dose-dependent manner ($p < 0.001$) (Fig 7). TNF-α secretion was also significantly inhibited by ITF 2357 ($p < 0.001$) and Tubastatin A ($p < 0.001$).

Induced T reg cells derived from RA patients were mixed with CFSE-labeled Teff cells at ratios of 1:1, 0.3:1 and 0:1. The mixed cells were incubated with vehicle or HDAC inhibitor (0.01 to 5 μM) in the presence of Dynabeads® human T-activator CD3/C28 (one bead to 4 cells) for 3 days. Proliferation of Teff cells was inhibited after treatment with CKD-L (5 μM) and ITF 2357 (0.1 μM) compared to vehicle (Fig 8a). As the proportion of induced Treg cells was increased, proliferation of Teff cells was inhibited. In addition, in the Teff cell only condition, ITF 2357 inhibited the proliferation of Teff cells but CKD-L did not have an effect. Therefore, the suppressive effect of CKD-L seems to be mediated by Treg cells. Tubastatin A had no suppressive effect in the suppression assay. The suppression ratio (fold versus vehicle) at 1:1 ratio of Treg:Teff was increased 1.5 times by CKD-L treatment and 1.8 times by ITF 2357 treatment compared to vehicle treatment ($p < 0.05$ and $p < 0.01$, respectively) (Fig 8b).

a)

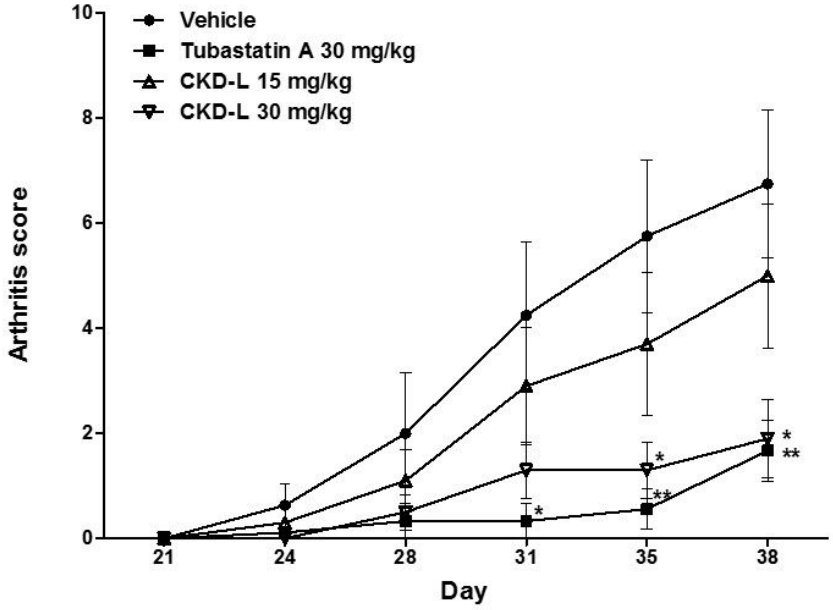
Vehicle
Tubastatin A 30 mg/kg
CKD-L 15 mg/kg
CKD-L 30 mg/kg
Arthritis score
Day
10
8
6
4
2
0
21
24
28
31
35
38
*
**
*
**
*
**

b)

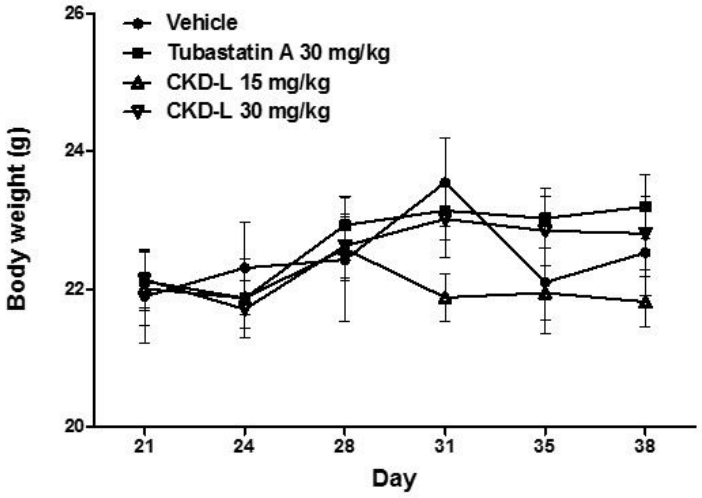
Vehicle
Tubastatin A 30 mg/kg
CKD-L 15 mg/kg
CKD-L 30 mg/kg
Body weight (g)
Day
26
24
22
20
21
24
28
31
35
38

c)

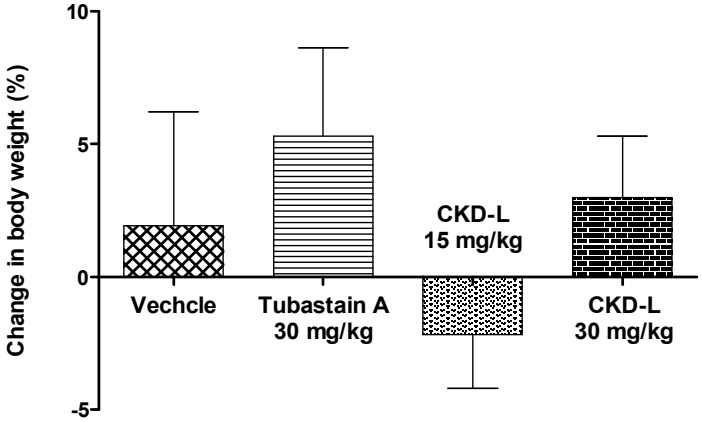

Figure 1. Therapeutic effects of CKD-L on CIA mice.

After the onset of arthritis, mice were treated with vehicle, Tubastatin A (30 mg/kg), or CKD-L (15 or 30 mg/kg) subcutaneously every day for 18 days after the second immunization. CKD-L (30 mg/kg) and Tubastatin A significantly decreased arthritis score compared to vehicle (a). Body weight did not change during drug administration (b). The changes in body weight between day 21 and day 38 was not significantly different among the groups.

$*p < 0.05$, $**p < 0.01$ vs. vehicle.

a)

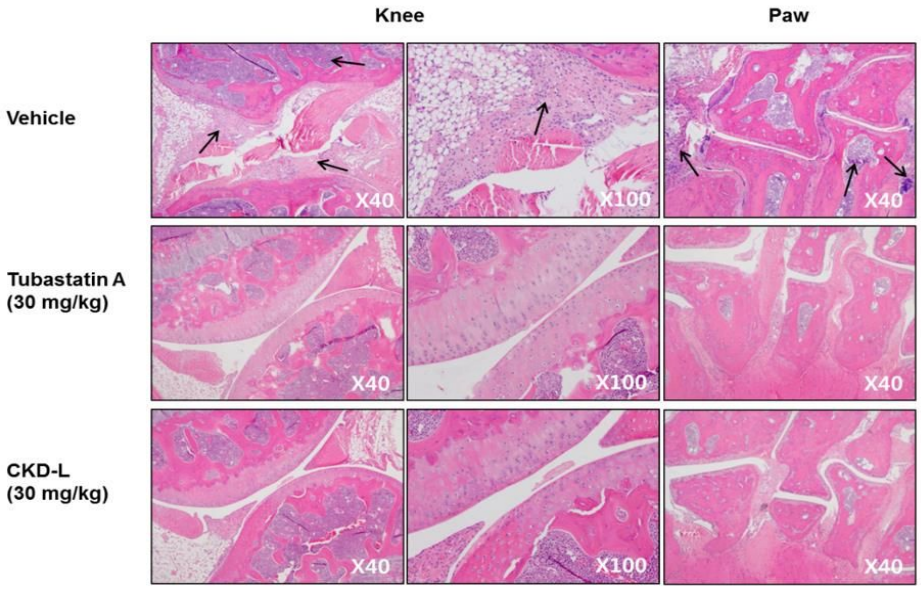
Knee
Paw
Vehicle
Tubastatin A
(30 mg/kg)
CKD-L
(30 mg/kg)
X40
X100
X40
X40
X100
X40
X40
X100
X40

b)

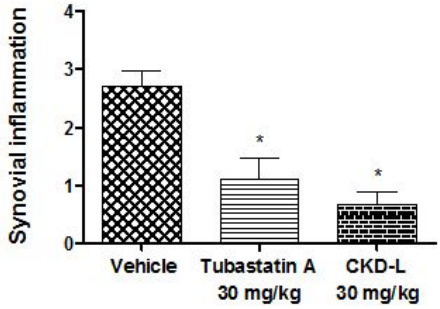
Synovial inflammation
4
3
2
1
0
*
*
Vehicle
Tubastatin A 30 mg/kg
CKD-L 30 mg/kg

c)

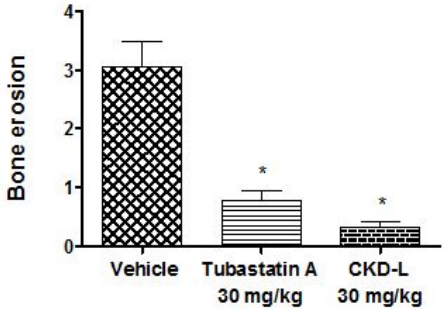
Bone erosion
4
3
2
1
0
*
*
Vehicle
Tubastatin A 30 mg/kg
CKD-L 30 mg/kg

d)

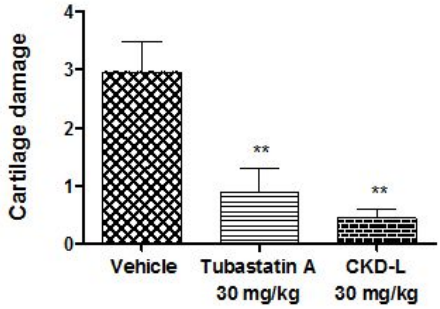
Cartilage damage
4
3
2
1
0
**
**
Vehicle
Tubastatin A 30 mg/kg
CKD-L 30 mg/kg

e)

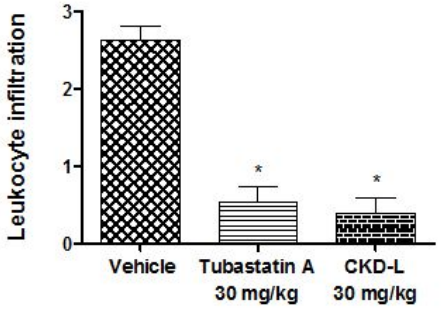
Leukocyte infiltration
3
2
1
0
*
*
Vehicle
Tubastatin A 30 mg/kg
CKD-L 30 mg/kg

f)

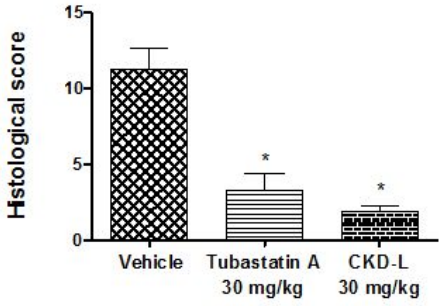
Histological score
15
10
5
0
*
*
Vehicle
Tubastatin A 30 mg/kg
CKD-L 30 mg/kg

Figure 2. Histological analysis of CIA treated with CKD-L or Tubastatin A.

Histological analyses were performed on knee joints (X40, X100) and hind paws (X40) stained by H&E. Synovial inflammation, bone erosion, cartilage damage, and leukocyte infiltration were observed in the knee joints and hind paws of mice treated with vehicle (arrow) compared to Tubastatin A or CKD-L (a). The mean score of synovial inflammation (b), bone erosion (c), cartilage damage (d), and leukocyte infiltration (e) were calculated using a scale of 0-4 (normal: 0, mild: 1, moderate: 2, marked: 3, severe: 4), and these parameters significantly decreased after CKD-L or Tubastatin A treatment compared to vehicle treatment. Histological score was calculated by summation of these parameters (f). Histological score significantly decreased following treatment with CKD-L or Tubastatin A.

$*p < 0.001$, $**p < 0.01$ vs. vehicle.

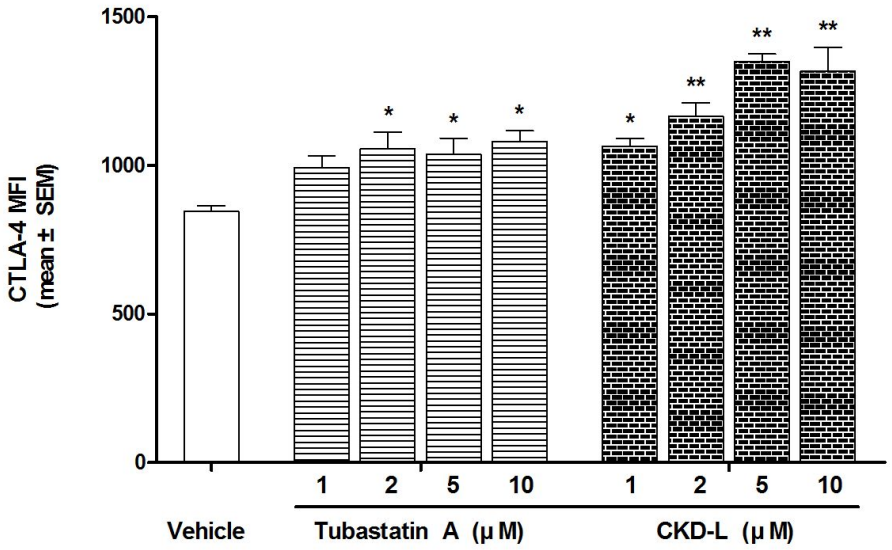

Figure 3. Increased CTLA-4 expression by CKD-L in Treg cells from C57BL/6 mice.

$CD4^+CD25^-$ T cells were isolated from splenocytes of C57BL/6 mice. $CD4^+CD25^-$ T cells were incubated with vehicle or HDAC6 inhibitors (1 to 10 μM) in the presence of anti-CD3/CD28 beads and recombinant TGF-β2 in a 48 well plate for 6 days. CTLA-4 expression in $CD4^+CD25^+Foxp3^+$ T cells was analyzed by mean fluorescence intensity (mean ± SEM) by using flow cytometry.

*$p < 0.05$, **$p < 0.001$ vs. vehicle.

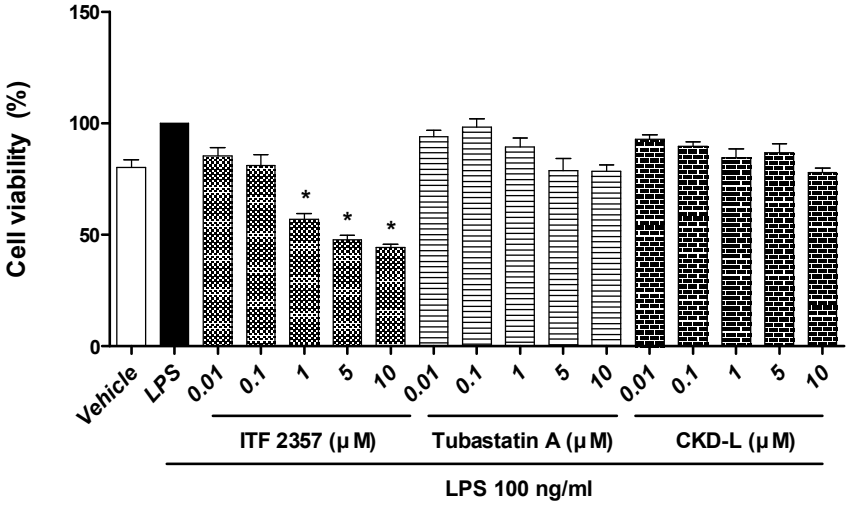

Figure 4. Effects of CKD-L on cell viability in PBMCs from RA patients (n=6).

PBMCs from RA patients were cultured in a 96 well plate for 24 hours in the presence of LPS (100 ng/ml) and HDAC inhibitors at different concentrations (0.01 to 5 μM). Cell viability was determined using the MTT assay. Bars represent means and SDs. All experiments were carried out in triplicate.

*$p < 0.001$ vs. LPS.

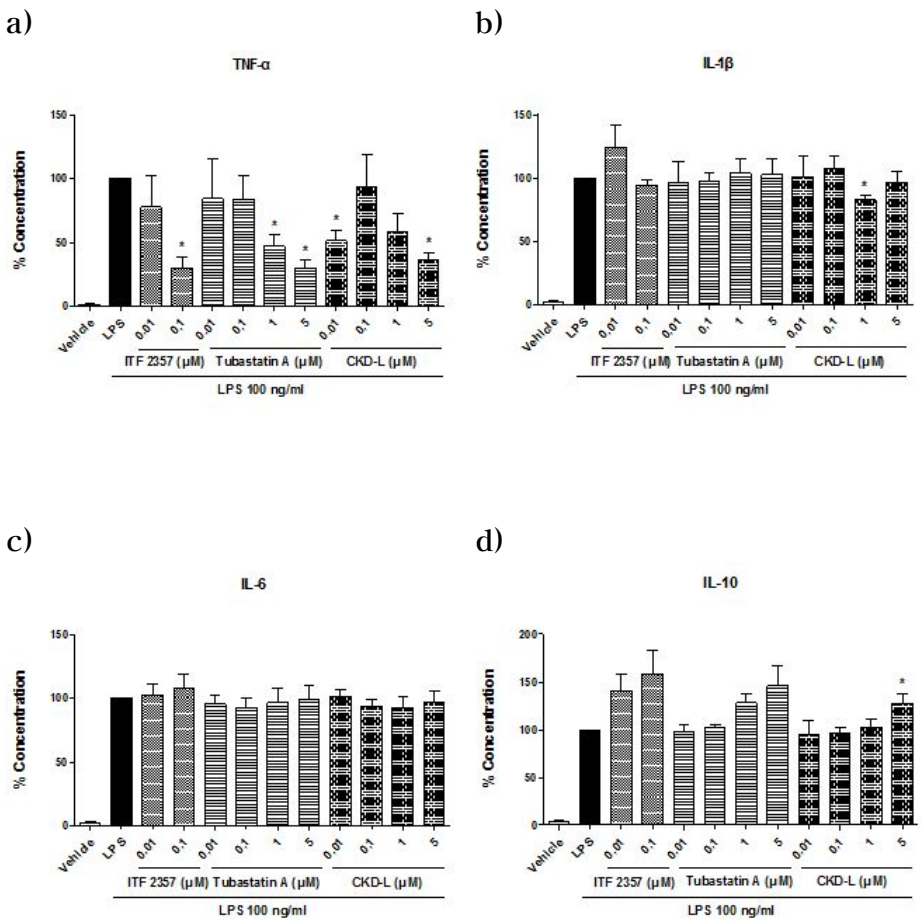

Figure 5. Effects of CKD-L on cytokine secretion in PBMCs from RA patients (n=5).

PBMCs from RA patients were cultured in a 48 well plate for 24 hours in the presence of LPS (100 ng/ml) and HDAC inhibitors at different concentrations (0.01 to 5 μM). TNF-α (a), IL-1β (b), IL-6 (c), and IL-10 (d) were measured in the culture supernatant by ELISA.

*$p < 0.01$ vs. LPS.

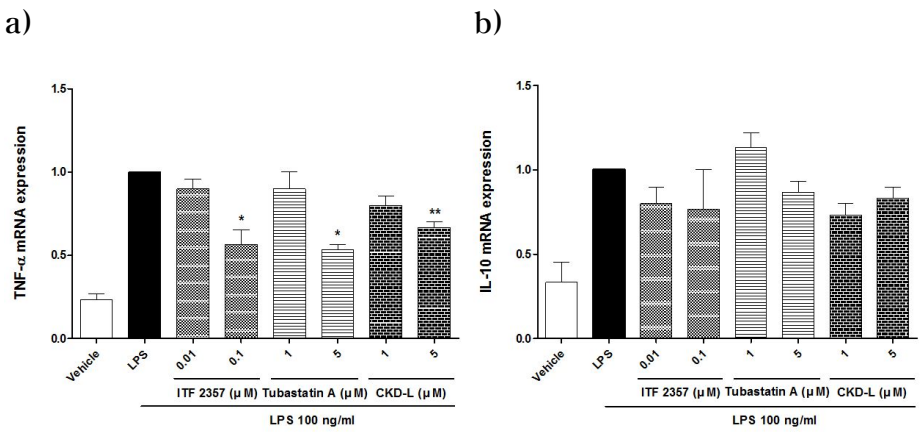

Figure 6. Effects of CKD-L on cytokine mRNA expression in PBMCs from RA patients (n=3).

PBMCs from RA patients were cultured in a 48 well plate for 24 hours in the presence of LPS (100 ng/ml) and HDAC inhibitors at different concentrations (0.01 to 5 μM). Total RNA was extracted from harvested cells and cDNA was synthesized by RT-PCR. TNF-α (a) and IL-10 (b) mRNA expression levels were analyzed by real-time PCR.

*p < 0.001, **p < 0.01 vs. LPS.

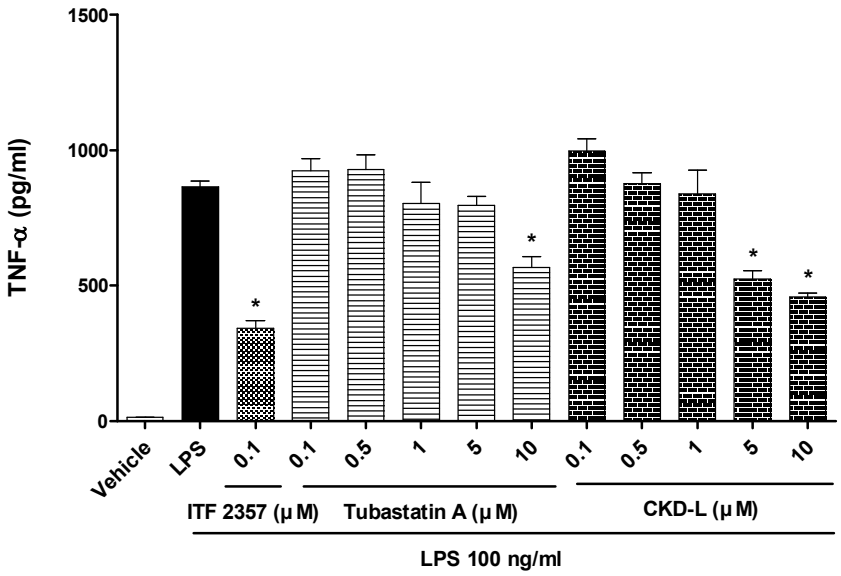

Figure 7. TNF-α secretion in PMA-activated THP-1 cells.
THP-1 cells ($1X10^5$ cells/well) were cultured in a 24 well plate and activated with PMA (10 ng/ml) for 24 hours to induce macrophage differentiation. PMA-activated THP-1 cells were treated with vehicle or HDAC inhibitors (0.1 to 10 μM) for 24 hours and then treated with 100 ng/ml LPS for 4 hours. The secretion of TNF-α was measured by ELISA.
*$p < 0.001$ vs. LPS.

a)

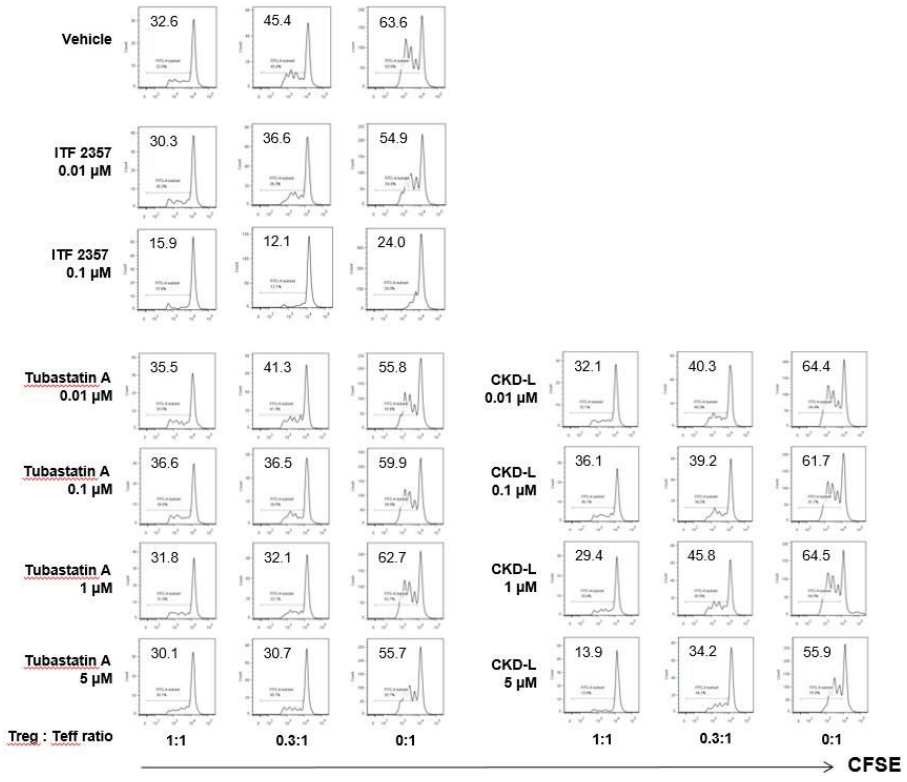
Vehicle
32.6
45.4
63.6
ITF 2357 0.01 µM
30.3
36.6
54.9
ITF 2357 0.1 µM
15.9
12.1
24.0
Tubastatin A 0.01 µM
35.5
41.3
55.8
Tubastatin A 0.1 µM
36.6
36.5
59.9
Tubastatin A 1 µM
31.8
32.1
62.7
Tubastatin A 5 µM
30.1
30.7
55.7
CKD-L 0.01 µM
32.1
40.3
64.4
CKD-L 0.1 µM
36.1
39.2
61.7
CKD-L 1 µM
29.4
45.8
64.5
CKD-L 5 µM
13.9
34.2
55.9
Treg : Teff ratio
1:1
0.3:1
0:1
1:1
0.3:1
0:1
CFSE

b)

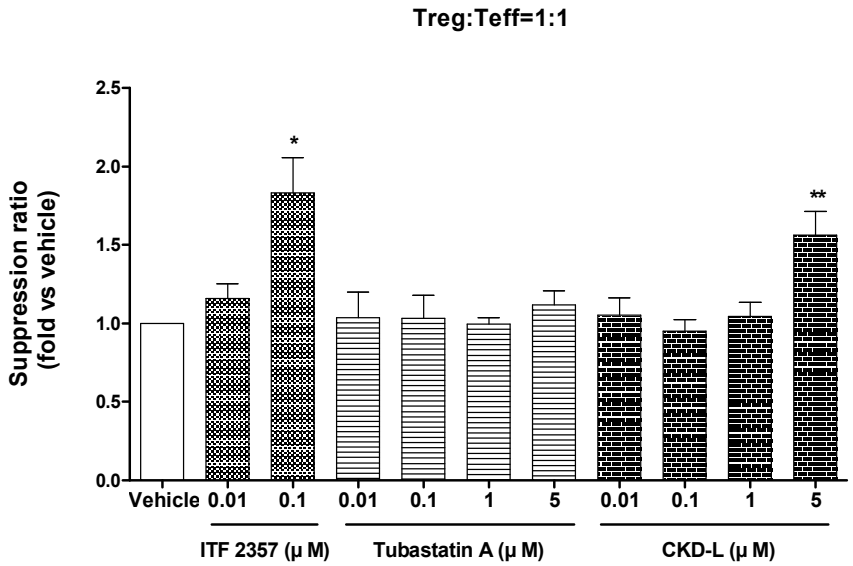

Figure 8. Effects of CKD-L in the suppression assay using induced Treg cells and Teff cells from RA patients.

Treg cells induced from RA patients were mixed with CFSE-labeled Teff cells at ratios of 1:1, 0.3:1 and 0:1. The mixed cells were incubated with vehicle or HDAC inhibitors (0.01 to 5 μM) in the presence of Dynabeads® human T-activator CD3/C28 (one bead to 4 cells) for 3 days. a) The proliferation of Teff cells was assessed by CFSE dilution using flow cytometry (representative data). b) Suppression ratio (fold inhibition of cell proliferation by HDACi vs. vehicle) at the ratio of Treg:Teff = 1:1.

*p <0.001, **p < 0.05.

Discussion

Epigenetic regulation potentially influences the pathogenesis of RA and can provide therapeutic targets for the treatment of RA [34]. HDAC inhibitors that modulate the activities of HDAC and HAT have been reported to have the potential anti-inflammatory effects on RA in many studies [5, 22-25]. In addition, HDAC inhibitors ameliorated joint inflammation and bone destruction in the animal experiments, including CIA model [3, 5]. Therefore, in the present study, we hypothesized that CKD-L could have beneficial effects on CIA. We found that CKD-L significantly decreased both arthritis score and histological score by blocking CIA progression.

We assessed the effect of CKD-L on the function of Treg cells. Treg cells and Teff cells were isolated from splenocytes of C57BL/6 mice and co-cultured. Proliferation of Teff cells was inhibited after treatment with CKD-L or Tubastatin A in a dose-dependent manner. The suppression ratio (fold inhibition of cell proliferation by HDACi vs. vehicle) was approximately two times greater after CKD-L treatment compared to vehicle treatment (data not

shown).

In RA, activated $CD4^+$ T cells have an important role in initiating and perpetuating chronic inflammation [35]. Based on their distinctive cytokine secretion profiles and functions, human $CD4^+$ T cells can be divided into two major subtypes of cells, known as Th1 and Th2 cells. Th1 cells produce the pro-inflammatory cytokines IFN-γ, TNF-α and IL-2, and promote macrophage activation, induce delayed-type hypersensitivity, and are involved in cell-mediated immunity. Th2 cells have been associated with down-regulation of macrophage effector functions, they produce the anti-inflammatory cytokines IL-4, IL-5, IL-10, and IL-13, and mediate allergic immune responses [35-37]. IgG2a production is associated with a Th1 response, whereas IgG1 production is associated with a Th2 response [38]. Therefore, we hypothesized that CKD-L can increase or maintain the level of IgG1 and decrease the level of IgG2a in serum from animals with CIA. We measured the levels of serum IgG1 and IgG2a by ELISA. However, the levels of serum IgG1 and IgG2a did not change significantly after CKD-L treatment (data not shown).

HDAC inhibitors have been reported to reduce the levels of TNF-α, IL-1α, IL-1β, and IFN-γ in LPS-

stimulated normal PBMCs and reduce the levels of pro-inflammatory cytokines such as TNF-α and IL-6 in PBMCs of RA patients [1, 24, 26, 28]. We found that CKD-L inhibited the secretion of TNF-α and IL-1β, and increased the secretion of IL-10 in PBMCs of RA patients treated with LPS and HDAC inhibitors. Also, as assessed by real-time PCR, CKD-L significantly inhibited TNF-α mRNA level, in accordance with the results of measurements taken from the cell culture supernatant. Tubastatin A and ITF 2357 inhibited TNF-α secretion, but had no effect on IL-1β or IL-10. CKD-L, which regulates several cytokines such as TNF-α, IL-1β, and IL-10, is expected to play an important role in abnormal immune responses in RA patients.

In RA, T cells and macrophages are major sources of pro-inflammatory cytokines and the activation, survival, and apoptosis of these cells may be regulated by HDAC and HAT [27]. It is known that HDAC inhibitors suppress TNF-α and IL-6 production and transcription of cytokines in macrophages, and induce apoptosis in macrophages [28]. We found that CKD-L inhibited TNF-α secretion in PMA-activated THP-1 in a dose-dependent manner. Increased histone acetylation can regulate TNF-α production by controlling the

access of transcription factors to promoter motifs directly or by regulating nucleosome remodeling.

Treg cells play an immunosuppressive role by producing TGF-β or inhibiting Teff cells [29]. Treg cells from RA patients are defective in the suppression of pro-inflammatory cytokine production [30]. TNF-α in RA decreases the immunosuppressive effect by inducing the malfunction of Treg cells. It is known that inhibition of HDAC6 enhances the suppressive activity of Treg cells in inflammation and autoimmunity [12]. In the present study, in C57BL/6 mice, CKD-L increased CTLA-4 expression in $CD4^+CD25^+Foxp3^+$ T cells more effectively than did Tubastatin A. In the suppression assay on PBMCs from RA patients, we found that CKD-L significantly inhibited the proliferation of Teff cells compared to vehicle. As the ratio of Treg cells increased, the proliferation of Teff cells was inhibited to a greater degree. Interestingly, ITF 2357 inhibited the proliferation of Teff cells when only Teff cells were present in culture. On the other hand, CKD-L had no effect when only Teff cells were present. Therefore, the suppressive effect of CKD-L seems to be regulated through Treg cells. Tubastatin A had no suppressive effect on suppression assay. These results suggest that

CKD-L promote the suppressive function of Treg cells. HDAC inhibitors can increase acetylation of histone and Foxp3, leading to increased expression of Foxp3, and increase the production and suppressive function of Treg cells [39]. Foxp3 proteins in Treg cells are present in a dynamic protein complex containing HAT and HDAC enzymes, and Foxp3 itself is acetylated on lysine residues. In addition, it has been reported that CTLA-4 expression is associated with acquisition of a suppressive function in activated human $CD4^{+}CD25^{-}$ T cells [40].

There are few studies on the comparative effect of selective versus nonselective HDAC inhibitors. HDAC6 has been reported to modulate many important biological processes, including cell migration, immune responses, viral infections and the degradation of misfolded proteins. These diverse functions of HDAC6 can be used as potential therapeutic targets in various diseases, such as systemic lupus erythematosus, cancer, and diabetes [10, 11]. Our data demonstrated that CKD-L, a selective HDAC6 inhibitor, decreased arthritis score and protected against joint destruction in the CIA model, and reduced the expressions of TNF-α and IL-1β, and increased the expression of IL-10 in PBMCs from RA patients. Also, CKD-L

increased CTLA-4 expression and the suppressive function of Treg cells. Our data suggest that CKD-L may have a beneficial effect in the treatment of RA and further studies are needed to establish its role as a potential therapeutic agent.

Reference

1. Gillespie J, Savic S, Wong C, Hempshall A, Inman M, Emery P, Grigg R and McDermott MF, Histone deacetylases are dysregulated in rheumatoid arthritis and a novel histone deacetylase 3-selective inhibitor reduces interleukin-6 production by peripheral blood mononuclear cells from rheumatoid arthritis patients. Arthritis Rheum, 2012. 64(2): p. 418-22.

2. Kim DH, Kim M and Kwon HJ, Histone deacetylase in carcinogenesis and its inhibitors as anti-cancer agents. J Biochem Mol Biol, 2003. 36(1): p. 110-9.

3. Joosten LA, Leoni F, Meghji S and Mascagni P, Inhibition of HDAC activity by ITF 2357 ameliorates joint inflammation and prevents cartilage and bone destruction in experimental arthritis. Mol Med, 2011. 17(5-6): p. 391-6.

4. Gregoretti IV, Lee YM and Goodson HV, Molecular evolution of the histone deacetylase family: functional implications of phylogenetic analysis. J Mol Biol, 2004. 338(1): p. 17-31.

5. Lin HS, Hu CY, Chan HY, Liew YY, Huang HP, Lepescheux L, Bastianelli E, Baron R, Rawadi G and Clement-Lacroix P, Anti-rheumatic activities of

histone deacetylase (HDAC) inhibitors in vivo in collagen-induced arthritis in rodents. Br J Pharmacol, 2007. 150(7): p. 862-72.
6. New M, Olzscha H and La Thangue NB, HDAC inhibitor-based therapies: can we interpret the code? Mol Oncol, 2012. 6(6): p. 637-56.
7. Kong Y, Jung M, Wang K, Grindrod S, Velena A, Lee SA, Dakshanamurthy S, Yang Y, Miessau M, Zheng C, Dritschilo A and Brown ML, Histone deacetylase cytoplasmic trapping by a novel fluorescent HDAC inhibitor. Mol Cancer Ther, 2011. 10(9): p. 1591-9.
8. Lee JH, Mahendran A, Yao Y, Ngo L, Venta-Perez G, Choy ML, Kim N, Ham WS, Breslow R and Marks PA, Development of a histone deacetylase 6 inhibitor and its biological effects. Proc Natl Acad Sci U S A, 2013. 110(39): p. 15704-9.
9. Li Y, Shin D and Kwon SH, Histone deacetylase 6 plays a role as a distinct regulator of diverse cellular processes. FEBS J, 2013. 280(3): p. 775-93.
10. Valenzuela-Fernandez A, Cabrero JR, Serrador JM and Sanchez-Madrid F, HDAC6: a key regulator of cytoskeleton, cell migration and cell-cell interactions. Trends Cell Biol, 2008. 18(6): p. 291-7.
11. Zhang X, Yuan Z, Zhang Y, Yong S, Salas-Burgos A, Koomen J, Olashaw N, Parsons JT, Yang XJ, Dent

SR, Yao TP, Lane WS and Seto E, HDAC6 modulates cell motility by altering the acetylation level of cortactin. Mol Cell, 2007. 27(2): p. 197-213.
12. de Zoeten EF, Wang L, Butler K, Beier UH, Akimova T, Sai H, Bradner JE, Mazitschek R, Kozikowski AP, Matthias P and Hancock WW, Histone deacetylase 6 and heat shock protein 90 control the functions of Foxp3(+) T-regulatory cells. Mol Cell Biol, 2011. 31(10): p. 2066-78.
13. Yamashita Y, Shimada M, Harimoto N, Rikimaru T, Shirabe K, Tanaka S and Sugimachi K, Histone deacetylase inhibitor trichostatin A induces cell-cycle arrest/apoptosis and hepatocyte differentiation in human hepatoma cells. Int J Cancer, 2003. 103(5): p. 572-6.
14. Marks PA, Richon VM and Rifkind RA, Histone deacetylase inhibitors: inducers of differentiation or apoptosis of transformed cells. J Natl Cancer Inst, 2000. 92(15): p. 1210-6.
15. Delcuve GP, Khan DH and Davie JR, Roles of histone deacetylases in epigenetic regulation: emerging paradigms from studies with inhibitors. Clin Epigenetics, 2012. 4(1): p. 5.
16. Bayarsaihan D, Epigenetic mechanisms in inflammation. J Dent Res, 2011. 90(1): p. 9-17.

17. Han GM, O'Neil-Andersen NJ, Zurier RB and Lawrence DA, $CD4^{+}CD25^{high}$ T cell numbers are enriched in the peripheral blood of patients with rheumatoid arthritis. Cell Immunol, 2008. 253(1-2): p. 92-101.
18. Gravallese EM, Bone destruction in arthritis. Ann Rheum Dis, 2002. 61 Suppl 2: p. ii84-6.
19. Edwards CJ and Cooper C, Early environmental factors and rheumatoid arthritis. Clin Exp Immunol, 2006. 143(1): p. 1-5.
20. Gaffo A, Saag KG and Curtis JR, Treatment of rheumatoid arthritis. Am J Health Syst Pharm, 2006. 63(24): p. 2451-65.
21. Feldmann M and Maini RN, Anti-TNF alpha therapy of rheumatoid arthritis: what have we learned? Annu Rev Immunol, 2001. 19: p. 163-96.
22. Blanchard F and Chipoy C, Histone deacetylase inhibitors: new drugs for the treatment of inflammatory diseases? Drug Discov Today, 2005. 10(3): p. 197-204.
23. Mishra N, Brown DR, Olorenshaw IM and Kammer G, Trichostatin A reverses skewed expression of CD154, interleukin-10, and interferon-gamma gene and protein expression in lupus T cells. Proc Natl Acad Sci U S A, 2001. 98(5): p. 2628-33.
24. Leoni F, Fossati G, Lewis EC, Lee JK, Porro G,

Pagani P, Modena D, Moras ML, Pozzi P, Reznikov LL, Siegmund B, Fantuzzi G, Dinarello CA and Mascagni P, The histone deacetylase inhibitor ITF 2357 reduces production of pro-inflammatory cytokines in vitro and systemic inflammation in vivo. Mol Med, 2005. 11(1-12): p. 1-15.

25. Chung YL, Lee MY, Wang AJ and Yao LF, A therapeutic strategy uses histone deacetylase inhibitors to modulate the expression of genes involved in the pathogenesis of rheumatoid arthritis. Mol Ther, 2003. 8(5): p. 707-17.

26. Grabiec AM, Korchynskyi O, Tak PP and Reedquist KA, Histone deacetylase inhibitors suppress rheumatoid arthritis fibroblast-like synoviocyte and macrophage IL-6 production by accelerating mRNA decay. Ann Rheum Dis, 2012. 71(3): p. 424-31.

27. Lacy P and Stow JL, Cytokine release from innate immune cells: association with diverse membrane trafficking pathways. Blood, 2011. 118(1): p. 9-18.

28. Grabiec AM, Krausz S, de Jager W, Burakowski T, Groot D, Sanders ME, Prakken BJ, Maslinski W, Eldering E, Tak PP and Reedquist KA, Histone deacetylase inhibitors suppress inflammatory activation of rheumatoid arthritis patient synovial macrophages and tissue. J Immunol, 2010. 184(5): p. 2718-28.

29. Esensten JH, Wofsy D and Bluestone JA, Regulatory T cells as therapeutic targets in rheumatoid arthritis. Nat Rev Rheumatol, 2009. 5(10): p. 560-5.
30. Nadkarni S, Mauri C and Ehrenstein MR, Anti-TNF-alpha therapy induces a distinct regulatory T cell population in patients with rheumatoid arthritis via TGF-beta. J Exp Med, 2007. 204(1): p. 33-9.
31. Brand DD, Latham KA and Rosloniec EF, Collagen-induced arthritis. Nat Protoc, 2007. 2(5): p. 1269-75.
32. Arnett FC, Edworthy SM, Bloch DA, McShane DJ, Fries JF, Cooper NS, Healey LA, Kaplan SR, Liang MH, Luthra HS, et al., The American Rheumatism Association 1987 revised criteria for the classification of rheumatoid arthritis. Arthritis Rheum, 1988. 31(3): p. 315-24.
33. Ehrenstein MR, Evans JG, Singh A, Moore S, Warnes G, Isenberg DA and Mauri C, Compromised function of regulatory T cells in rheumatoid arthritis and reversal by anti-TNFalpha therapy. J Exp Med, 2004. 200(3): p. 277-85.
34. Viatte S, Plant D and Raychaudhuri S, Genetics and epigenetics of rheumatoid arthritis. Nat Rev Rheumatol, 2013. 9(3): p. 141-53.
35. Skapenko A, Wendler J, Lipsky PE, Kalden JR and

Schulze-Koops H, Altered memory T cell differentiation in patients with early rheumatoid arthritis. J Immunol, 1999. 163(1): p. 491-9.
36. Del Prete GF, De Carli M, Ricci M and Romagnani S, Helper activity for immunoglobulin synthesis of T helper type 1 (Th1) and Th2 human T cell clones: the help of Th1 clones is limited by their cytolytic capacity. J Exp Med, 1991. 174(4): p. 809-13.
37. Seder RA and Paul WE, Acquisition of lymphokine-producing phenotype by $CD4^+$ T cells. Annu Rev Immunol, 1994. 12: p. 635-73.
38. Apparailly F, Verwaerde C, Jacquet C, Auriault C, Sany J and Jorgensen C, Adenovirus-mediated transfer of viral IL-10 gene inhibits murine collagen-induced arthritis. J Immunol, 1998. 160(11): p. 5213-20.
39. Tao R, de Zoeten EF, Ozkaynak E, Chen C, Wang L, Porrett PM, Li B, Turka LA, Olson EN, Greene MI, Wells AD and Hancock WW, Deacetylase inhibition promotes the generation and function of regulatory T cells. Nat Med, 2007. 13(11): p. 1299-307.
40. Zheng Y, Manzotti CN, Burke F, Dussably L, Qureshi O, Walker LS and Sansom DM, Acquisition of suppressive function by activated human $CD4^+$ $CD25^-$ T cells is associated with the expression of CTLA-4 not FoxP3. J Immunol, 2008. 181(3): p. 16835213-91.

국문 초록

콜라겐 유도 관절염 동물모델과 류마티스 관절염 환자의 조절 T 세포에서 새로운 히스톤 탈아세틸화효소 6 억제제, CKD-L의 치료 효과

서울대학교 융합과학기술대학원
분자의학 및 바이오제약학과
오보람

배경: 히스톤 탈아세틸화효소와 히스톤 아세틸화효소에 의해서 조절되는 후성유전학은 류마티스 관절염을 포함한 염증성 관절염에서 중요한 역할을 한다. 류마티스 관절염은 만성 자가면역 질환으로 염증성 활막염과 통증, 붓기, 기능 손실로 이어지는 관절 연골과 뼈의 점진적인 파괴를 특징으로 한다. 히스톤 탈아세틸화효소 억제제는 최근 관절염 동물모델에서 항 염증성 제제로 치료 효과를 갖는 것으로 보고되었다.

목적: 본 연구에서는 콜라겐 유도 관절염 동물모델과 류마티스 환자의 조절 T세포에서 새로운 선택적 히스톤 탈아세틸화효소 6 억제제인 CKD-L의 효과를 분석하고 ITF 2357 (범 HDAC 억제제)과 Tubastatin A (선택적 HDAC6 억제제)와 비교하였다.

방법: 콜라겐 유도 관절염 동물 모델은 DBA/1J 생쥐에 우형 제 2 형 콜라겐을 이용하여 유도하였다. 생쥐는 대조군 (10 마리), CKD-L (15, 30 mg/kg, 각각 10 마리), Tubastatin A (30 mg/kg, 9 마리)를 18일 동안 매일 피하주사 하였다. 관절염 지수는 관절염 발병 후 매주 2번씩 측정되었다. 조직병리학적 분석은 H&E 염색을 이용하였다.

$CD4^+CD25^-$ T 세포는 C57BL/6 생쥐 비장에서 분리하였고 항 CD3/CD28 비드, TGF-β와 탈아세틸화효소 6 억제제 (1~10 μM)로 6일 동안 배양하였다. 유도된 조절 T 세포의 CTLA-4 발현은 유세포 분석을 이용하여 측정하였다.

류마티스 환자의 말초혈액 단핵세포는 LPS와 탈아세틸화효소 억제제 (ITF 2357, 0.01 to 0.1 μM, CKD-L and Tubastatin A, 0.01 to 5 μM)와 함께 24 시간 동안 배양하였다. TNF-α, IL-10, IL-1β와 IL-6의 분비는 효소면역측정법을 이용하여 세포 상층액에서 측정하였다. TNF-α와 IL-10의 mRNA 발현은 실시간 중합효소연쇄반응으로 분석하였다.

THP-1 세포는 대식세포로 분화시키기 위해 PMA로 24시간 동안 활성화시켰다. PMA로 활성화된 THP-1 세포는 탈아세틸화효소 억제제와 24시간 동안 배양된 후, LPS 100 ng/ml 로 4시간 동안 배양되었다. TNF-α의 분비는 효소면역측정법으로 측정하였다.

류마티스 환자의 $CD4^+CD25^-$ T 세포는 항 CD3 항체, 항 CD28 항체, IL-2, TGF-β, 1,25-dihydroxyvitamin D_3와 함께 5일 동안 배양하였다. 유도된 조절 T 세포는 항 CD3/CD28 비드, 탈아세틸화효소 억제제 (ITF 2357, 0.01 to 0.1 μM, CKD-L

and Tubastatin A, 0.01 to 5 μM), CFSE로 표지된 효과 T 세포와 함께 3일 동안 배양하였다. 효과 T 세포의 증식은 유세포 분석으로 측정하였다.

결과: 콜라겐 유도 관절염 동물 모델에서 CKD-L과 Tubastatin A는 관절염 지수와 (CKD-L, $p < 0.05$, Tubastatin A, $p < 0.01$) 와 조직학적 지수 (CKD-L and Tubastatin A, 각각 $p < 0.001$)를 유의하게 감소시켰다. 생쥐 $Foxp3^+$ T 세포의 CTLA-4 발현은 CKD-L ($p < 0.001$)과 Tubastatin A ($p < 0.05$)를 처리하였을 때 유의하게 증가되었다.

류마티스 관절염 환자의 말초혈액 단핵세포에서 CKD-L은 TNF-α와 IL-1β를 억제하였고, IL-10을 증가시켰다. ITF 2357과 Tubastatin A는 TNF-α를 억제하였고, IL-1β와 IL-10에는 영향이 없었다. IL-6는 어떠한 탈아세틸화효소 억제제에도 변함이 없었다. 또한 CKD-L ($p < 0.01$), ITF 2357 ($p < 0.001$), Tubastatin A ($p < 0.001$)는 TNF-α의 mRNA 발현을 유의하게 억제하였다.

PMA 활성화된 THP-1 세포에서 분비하는 TNF-α는 CKD-L ($p < 0.001$)또는 Tubastatin A ($p < 0.001$)를 처리하였을 때 감소되었다.

유도된 조절 T 세포와 효과 T 세포의 공배양에서 효과 T 세포의 증식은 CKD-L 또는 ITF 2357에 의해 억제되었다. 조절 T 세포의 비율을 더 증가시키면 효과 T 세포의 증식이 더 억제되었다. Tubastatin A는 증식 억제에 효과가 없었다.

결론: 새로운 선택적 탈아세틸화효소 6 억제제인 CKD-L은 콜라겐 유도 관절염 동물 모델에서 관절염 지수를 감소시키고, 류마티스 관절염 환자의 PBMC에서 TNF-α와 IL-1β의 발현을 감소시키고 IL-10의 발현을 증가시켰다. 또한 CKD-L은 CTLA-4의 발현과 조절 T 세포의 억제 기능을 증가시켰다. 따라서 CKD-L은 류마티스 관절염 치료에 유익한 효과를 보일 것으로 사료된다.

주요어: 히스톤 탈아세틸화효소, 히스톤 탈아세틸화효소 억제제, 류마티스 관절염, 콜라겐 유도 관절염, 조절 T 세포

학 번: 2011-24246